

Modelling of the pendulum-driven cart system with friction

Wenjuan Ren (MRes student), Sam Wane (PhD student), and Hongnian Yu

Faculty of Computing, Engineering and Technology, Staffordshire University, Stafford, UK

rwenjuan@126.com, {S.O.Wane, H.Yu}@staffs.ac.uk

Abstract — This paper investigates several general friction models and applies different friction models to accurately simulate the propulsion of a capsule driven by an internally oscillating mass. The six published friction models are reviewed and are validated using the simulation studies. The simulation results are verified with a physical prototype in an experimentation test. The most accurate friction model can be chosen for a given application.

Keywords-Pendulum-driven cart, friction models, friction measurement experiment

I. INTRODUCTION

Friction is the resistance to motion that exists when a solid object is moved tangentially with respect to the surface of another that it touches, or when an attempt is made to produce such motion [1]. This is a common physical nonlinear phenomenon and exists in almost every kind of mechanical system and makes an effect on the system which cannot be ignored. Friction can lead to tracking errors, limit cycles and unsteady stick-slip movements [2]. If we do not minimize the friction force effectively, it may cause both economic losses and industrial losses. Friction is also a quite important factor to some processes, such as walking, starting and stopping a car, skating and so on.

Nowadays many focused researches are conducted on the ‘Capsule Robot’ for medical purposes, because the capsule robot can go into the human body to do work such as treatment, inspection, image acquisition and so on without hurting the patient [3], [4], [5]. A new tracking control issue via the pendulum-driven cart system was solved by the closed-loop control strategy [6]. The six-step optimization motion control approach was also improved by the pendulum-driven cart-pole system [7]. In [6] and [7], the velocity of the cart changed to negative value at some moment, so the displacement decreased. In the pendulum-driven cart system, there was no opposite force, the cart should not go backwards, and this paper is to do research on this problem. However, a simple friction model was used in [3]-[7]. The friction plays an active role in the capsule robot movement. This paper aims to investigate the realistic friction models which can be used in analysis and control of an active driving capsule robot.

This work has been supported by the European Erasmus-Mundus Sustainable eTourism project 2010-2359, the EPSRC UK-Japan Network on Human Adaptive Mechatronics Project (EP/E025250/1) and EU Erasmus Mundus Project-ELINK (EM ECW-ref.149674-EM-1- 2008-1-UK-ERAMUNDUS).

The structure of the paper is as follows: in section II, the review of previous work on the pendulum-driven cart pole-system is presented. In section III, investigation on friction phenomena and friction models are shown. A simulation study is carried out in section IV along with the implementation of the different friction models mentioned above. The experiment on measurement of friction parameters is described and compared with the experimental results and the simulation results, where the most suitable friction model for this system is selected. In section V, the conclusions are presented.

II. MODELLING OF THE PENDULUM-DRIVEN CART SYSTEM

Fig.1 shows the pendulum-driven cart system, the inverted pendulum is fixed on the cart. The cart has a relative smooth surface which makes it move horizontally on the ground. There is a torque motor mounted on the cart which generates the torque to swing the inverted pendulum. M is the mass of the cart, m is the mass of the ball of the pendulum, l is the length of the pendulum, μ is the friction coefficient between the ground and the cart, θ is the pendulum angle from the vertical direction, x is the displacement of the cart, and τ is the torque from the torque motor.

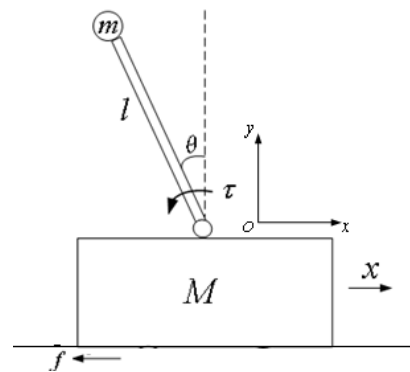


Figure 1. Pendulum-driven cart system

The Coulomb model of friction used in [6] is

$$F_f = -\mu N \operatorname{sgn}(\dot{x}), N = Mg + F_y \quad (1)$$

where μ is the friction coefficient between the cart and the surface, N is the normal force, F_y is the resultant force in the vertical direction.

The dynamic model of the system is described by

$$(M+m)\ddot{x} - ml\ddot{\theta}(\mu \sin \theta \operatorname{sgn} \dot{x} + \cos \theta) + ml\dot{\theta}^2(\sin \theta - \mu \cos \theta \operatorname{sgn} \dot{x}) + \mu(M+m)g \operatorname{sgn} \dot{x} = 0 \quad (2)$$

The improved friction model used in [7] is

$$F_f = -\mu N \operatorname{sgn}(\dot{x}), \quad N = Mg + F_y, \quad (3)$$

$$\mu = \begin{cases} \operatorname{sign}(F_x)\mu_k & (\dot{x} = 0) \\ \operatorname{sign}(\dot{x})\mu_k & (\dot{x} \neq 0) \end{cases}$$

where μ_k is the friction coefficient, F_y is the resultant force in the vertical direction. The following dynamic model can be obtained

$$(M+m)\ddot{x} - ml\ddot{\theta}(\mu \sin \theta + \cos \theta) + ml\dot{\theta}^2(\sin \theta - \mu \cos \theta) + \mu(M+m)g \operatorname{sgn} \dot{x} = 0 \quad (4)$$

Based on the friction model (2) and the dynamic model (4), the simulation was carried out using Matlab/Simulink and the sample time is 0.01 second. When the inverted pendulum swings, the reaction force from the pendulum to the cart drives the cart to move in the horizontal direction, the displacement of the cart is shown in Fig. 2.

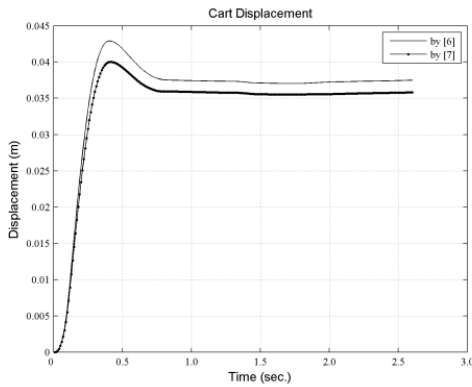


Figure 2. Cart displacements as found by [6] and [7]

From Fig. 2, there is decrease in the displacement curves, which means that the velocities of the cart change to negative values at the point that the displacement values decrease, which is not consistent with the reality situation, based on research of the reasons, improvement of the friction model can get the better result.

From the system configuration, the motor swings the pendulum to cause a lateral force on the cart to enable motion, which can be considered to be a spring. Assuming the cart to be a steel block on a smooth aluminium surface, the system can be simplified as shown in Fig. 5.

III. FRICTION MODELS

Friction is the key factor to determine the progress of the pendulum-driven cart and the accuracy between the simulation and the physical system. In this paper, general friction phenomena and friction models have been investigated and the friction models have been applied to the dynamic model of the pendulum-driven cart system in Matlab\ Simulink [6], [7] and physical experiment has been carried out to prove the real friction model of the system via

comparison of the simulation study and the experiment results.

Friction is the tangential reaction force between two surfaces in contact [8], is dependent on the physical characteristics of the contact surfaces, and displacement and the velocity of the contact body. There are many typical phenomena of friction, for instance, the Stribeck affect, hysteresis, spring-like characteristics for static friction, and varying break-away force [2]. Based on these friction phenomena, there are many friction models. The classical friction models are Coulomb friction model, Coulomb plus viscous friction model and Coulomb plus viscous plus static friction model [9].

Based on the experiment results, the Dahl friction model, LuGre friction model and so on [9], [10], [11] were proposed. In this paper, the Coulomb friction model, the Coulomb plus viscous friction model, the Coulomb plus viscous plus static friction model, the Stribeck friction model, the LuGre friction mode and the Dahl friction model are studied and implemented into the dynamic model of the pendulum-driven cart-pole system.

A. Modelling idea and evaluation criteria

The conventional hypothesis to model the friction is that the direction of the friction force should be opposite to the direction of the relative velocity between the two contact surfaces. In [6], [7], the velocity of the cart changes to negative and the cart retreats at the end of the motion. The reason for this is that at the moment when the velocity of the cart changes to zero, friction changes its direction to the opposite at once. However in the simulation study, it cannot be achieved exactly even if the sample time is very small, to save the computing time and get the more exact result, modelling the friction force under the new hypothesis that the friction tries to stop the mass block [12]. This paper switches the dynamic and static friction model when the relative velocity between the steel mass block and the aluminium surface changes to zero. The reason for switching is that when a body is moving, the friction involved is the dynamic friction, when the velocity of the body changes to zero, the body stops, at this time, the friction involved is the static friction. Consequently, the friction model in this paper is dynamic model when the velocity of the block is not equal to zero, and uses the static model when the velocity of the block changes to zero.

To select the most accurate friction model for the mass block system, evaluation criteria used in this paper are that the velocity will not change to negative and the displacement of the mass block will not decrease, that is, the mass block will stop with the effect of friction and there is no reverse motion in the system, which is consistent with the physical reality.

B. Friction phenomena

1) Stick-slip motion

Stick-slip motion is one of the typical friction behaviours in system. The reason for stick-slip motion is the friction is greater when the body keeps still than in motion, experiment [2] shows that the mass is still at first, and when there is a

linearly increasing force generated by the spring, the mass moves to a very small displacement firstly and then starts to slide when the applied force reaches the break-away force, decrease the spring force and the mass slows down and stops, the friction force increases because the static friction is greater than the dynamic friction. In [18], the model for stick-slip friction is always the function of velocity. Outside the small region around velocity is zero, the stick-slip friction is an arbitrary function of velocity, and inside the region, friction is determined by other forces in the system.

2) Stribeck effect

The Stribeck effect is to describe the friction behaviour when the relative velocity between the two contact surfaces is very small. The Stribeck friction force is function of steady-state velocity, when the relative velocity is within very low range, the friction force will decrease as the relative velocity increases. The relationship of the Stribeck effect and the relative velocity is shown in Fig. 3.

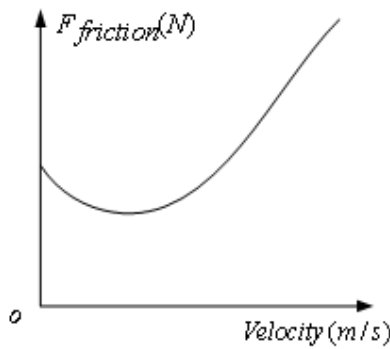


Figure 3. Stribeck effect

3) Pre-sliding displacement

When the applied force is smaller than the maximum static friction, the two contact bodies keep still, but from a micro point of view, there is a very tiny displacement on the asperities on the contact surfaces, this is called pre-sliding displacement, which is also known as the Dahl effect [9], [10]. During the pre-sliding stage of the contact bodies, the deflection of the asperities of the surfaces has the spring-like characteristic, and the friction force is the function of the displacement and is independent with the relative velocity between the contact surfaces. The graph of the Dahl effect and the displacement is shown as Fig. 4.

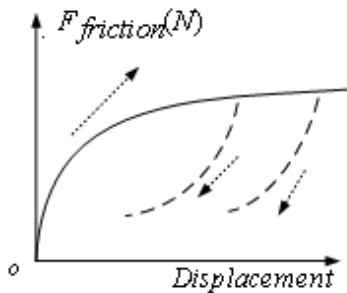


Figure 4. Pre-sliding displacement behaviour as found by [13]

C. Friction models

1) Stribeck model

The Stribeck model describes the friction phenomenon that the friction force does not decrease discontinuously when the contact surfaces starts to slip. The friction force is dependent on the velocity, when the relative velocity between the contact surfaces is very low, the friction force has a negative slope.

$$F = \begin{cases} F(v) & (\dot{x} \neq 0) \\ F_e = F_x & (\dot{x} = 0 \text{ \& } |F_e| < |F_s|) \\ F_s \operatorname{sgn}(F_e) & (\text{otherwise}) \end{cases} \quad (5)$$

$$F_v = F_c + (F_s - F_c) e^{-\frac{\dot{x}}{\dot{x}_s}} + \mu \dot{x}$$

where F_y is the Stribeck friction force, F_s is the static friction force, \dot{x}_s is called the Stribeck velocity, which means the low velocity as shown in Fig. 3[8], F_c is the Coulomb friction force, F_x is the resultant force in the horizontal direction.

2) Dahl friction model

The applied force is performed by the spring-like characteristics. There is a kind of viscous between the contact surfaces, if the applied force is larger than the defined range, and the viscous effect will be damaged.

$$\frac{dz}{dt} = \dot{x} - \sigma_0 \frac{|\dot{x}|}{F_c} Z$$

$$F_f = \begin{cases} F_d = \sigma_0 Z \operatorname{sgn}(\dot{x}) & (\dot{x} \neq 0) \\ F_x & (\dot{x} = 0) \end{cases} \quad (6)$$

where F_d is the Dahl friction force, F_c is the Coulomb friction force, σ_0 is the stiffness coefficient, and Z is the bristle deflection. When the velocity changes to zero, the friction form changes to the resultant force of the horizontal direction, that is F_x .

3) Coulomb friction model

The Coulomb friction model was discovered by Leonardo da Vinci (1452-1519) and is commonly used in engineering [14]. The Coulomb friction is opposite to the motion direction, proportion to the normal pressure, and independent with displacement, but dependent on the direction of velocity.

$$F_f = \begin{cases} F_c = \mu N \operatorname{sgn}(\dot{x}) & (\dot{x} \neq 0) \\ F_x & (\dot{x} = 0) \end{cases} \quad (7)$$

where μ is the friction coefficient, N is the normal force, \dot{x} is the velocity and F_x is the horizontal resultant force.

4) Viscous friction model

With the development of fluid dynamic technology, affect of viscosity lubrication and viscosity on force has been studied, and velocity has been considered as an important

factor of friction, the viscous friction model has been proposed as F_v in (8) [15], where \dot{x} is the sliding speed, and μ_v is the viscous coefficient. When the velocity changes to zero, the friction model switches to F_x as shown in (8).

$$F_f = \begin{cases} F_v = \mu_v \dot{x} \operatorname{sgn}(\dot{x}) & (\dot{x} \neq 0) \\ F_x & (\dot{x} = 0) \end{cases} \quad (8)$$

where F_v is the viscous friction, μ_v is the viscous friction coefficient, F_x is the resultant force in the horizontal direction, \dot{x} is the velocity.

5) LuGre friction model

The LuGre friction models the average deflection force of elastic springs [16]. If the applied tangential force is large enough to damage the spring-like characteristic, the bristle starts to slip. The LuGre friction models the Stribeck effect and supposes that the contact surfaces are pushed apart by the lubricant.

$$\begin{aligned} \frac{dz}{dt} &= \dot{x} - \frac{\sigma_1 |\dot{x}|}{F_v} Z \\ F_v &= F_c + (F_s - F_c) e^{-\left(\frac{\dot{x}}{v_s}\right)^\alpha} \\ F_f &= \begin{cases} F_v = (\sigma_1 Z + \sigma_2 \frac{dz}{dt} + \sigma_3 \dot{x}) \operatorname{sgn}(\dot{x}) & (\dot{x} \neq 0) \\ F_x & (\dot{x} = 0) \end{cases} \end{aligned} \quad (9)$$

where the state Z represents the average bristle deflection, which means the difference between the relative position of the bristle and the position where the bond was formed [8], σ_1 is the stiffness, σ_2 is the micro damping and σ_3 is the viscous friction coefficient, F_v represents the Stribeck effect, F_c is the Coulomb friction force and F_s is the static friction force.

6) Coulomb+viscous friction model

Based on the development of fluid mechanics, it is found that there is viscosity between the contact surfaces, the viscous friction force is proportional to the velocity.

$$F_f = \begin{cases} F_c \operatorname{sgn}(\dot{x}) + \mu \dot{x} \operatorname{sgn}(\dot{x}) & (\dot{x} \neq 0) \\ F_x & (\dot{x} = 0) \end{cases} \quad (10)$$

where F_c is the Coulomb friction, \dot{x} is the velocity, μ is the viscous friction coefficient and F_x is the resultant force in the horizontal direction.

IV. SIMULATION STUDY OF THE SPRING-BLOCK SYSTEM

To get the real values of the parameters, for instance, the dynamic friction coefficient, the static friction coefficient, the maximum static friction force and so on, in this paper, a physical experiment was carried out to complete this work.

For the system as shown in Fig. 5, the steel block stands on the aluminium flat, compasses the spring one end of

which is fixed to the left wall. When the spring is released, the steel block will move forward and will stop at one point because of the friction of the contact surfaces. Applying different friction models in simulation, different values of the mass block displacements can be obtained. The model under which the displacement value is closest to the experiment result can be chosen as the most accurate model.

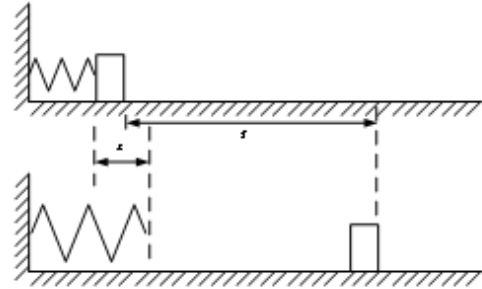


Figure 5. Spring-steel block system for experiment and simulation study

From the energy equation (11), the displacement of the system is unique for the determinant parameters. As a result, the value of displacement can be chosen as the key factor to select the friction model.

$$\frac{1}{2} kx^2 = \mu mg s \quad (11)$$

Both in the simulation study and in the experiment, the applied force is $F=10\text{N}$, the applied time is 0.1s.

TABLE I. STEEL BLOCK PARAMETERS

| Parameter | Value |
|-----------|----------|
| M | 1kg |
| K | 100N/m |
| μ_d | 0.25[17] |
| μ_s | 0.35[17] |

Parameters used simulation study, the same with the real parameters used in experiment

A. Physical experiment to find the most accurate friction model

As shown in Fig. 5, the spring is attached to the left wall with a compression length x . There are also a steel mass block and an aluminium platform. When the spring is released, the steel mass block will go to the right direction and will stop at a distance s . Values of parameters applied in the experiment and the simulation study are the same. In Fig. 5, m is the mass of the steel block, k the spring constant, and $F=Kx$ the external applied force to the system. The task of the experiment is to measure the displacement of the block when the spring releases. Parameter values used in the experiment are as shown in Table I. Through the experiment, the displacement of the mass block is $0.20m$.

B. Apply friction models to the spring-mass block system in simulink

1) *Coulomb friction model result*

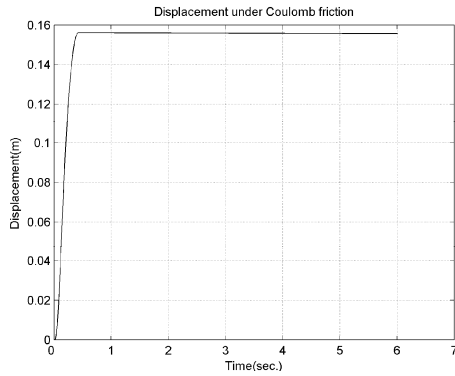


Figure 6. Displacement under Coulomb friction model

Figure 6. shows that the velocity of the mass block under the Coulomb friction model is always positive and the displacement keeps at 0.16m when the mass block goes to still, without reverse motion.

2) *Dahl friction model result*

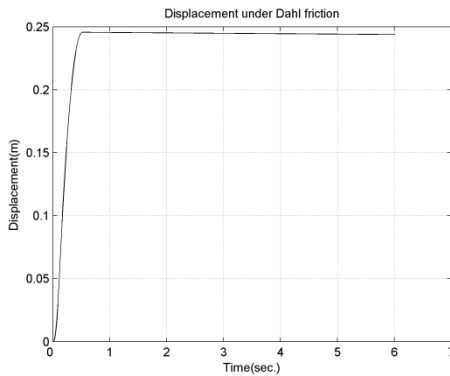


Figure 7. Displacement under Dahl friction model

Figure 7. illustrates that the relative velocity between the steel mass block and aluminium flat does not turn to negative, and the displacement is 0.25m when the steel block stops without the inverse motion.

3) *Stribeck friction model result*

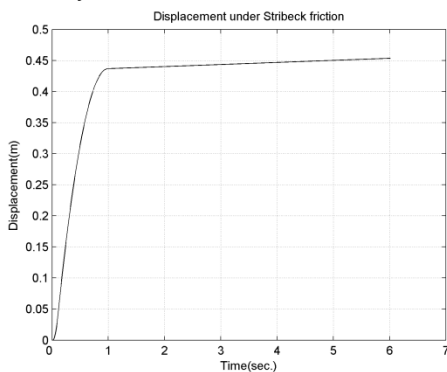


Figure 8. Displacement under Stribeck friction model

From Fig. 8, the velocity of the steel block under the Stribeck friction model does not change to zero exactly and the displacement is about 0.45m when the simulation time reaches about 10s, the final result is not consistent with the physical reality.

4) *LuGre friction model result*

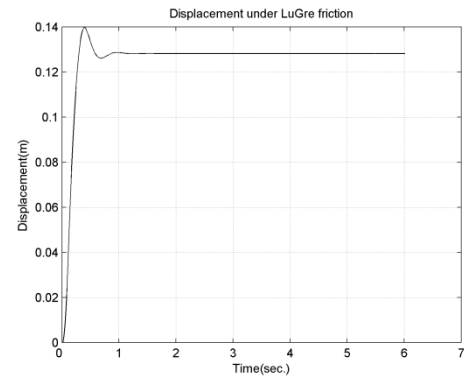


Figure 9. Displacement under LuGre friction model

Figure 9. demonstrates that the velocity of the steel block under the LuGre friction model firstly changes to negative and then returns to zero. And the displacement decreases before it keeps still. The final displacement is 0.13m.

5) *Coulomb plus viscous friction model result*

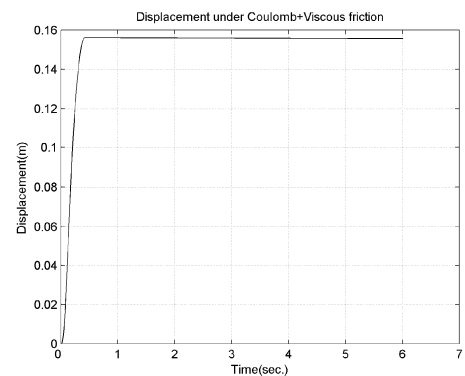


Figure 10. Displacement under Coulomb+Viscous friction model

From Fig. 10, the velocity does not change to negative and the displacement of the steel mass block stops at 0.16m without inverse motion.

The research results from the simulation study are summarized in table II.

TABLE II. RESEARCH RESULTS

| Friction model | Velocity* | Displacement | Relative error** |
|-----------------|-----------|--------------|------------------|
| Coulomb | Yes | 0.16m | 20% |
| Dahl | Yes | 0.25m | 25% |
| LuGre | No | 0.13m | 35% |
| Stribeck | Yes | 0.45m | 125% |
| Coulomb+Viscous | Yes | 0.16m | 20% |

*velocity is always positive or not; **relative error is between the simulation result and the experiment result.

From Table II, the LuGre friction model falls into disuse firstly because of negative velocity. Displacement of mass block reaches different values under different friction models. The minimal relative error is 20% under the improved Coulomb friction model as shown in (7) and improved Coulomb plus viscous friction model as shown in (10). According to the selection criterion proposed previous, the most accurate friction model should be the improved Coulomb friction model or the Coulomb plus viscous friction model.

Friction property depends mostly on the contact surfaces. Because the spring-steel block and the pendulum-driven cart share the same physical condition, the selected friction model can be applied to the pendulum-driven cart system in the future research.

V. CONCLUSIONS

Applying the selected friction model (take Coulomb plus viscous friction model for instance) to the pendulum-driven cart-pole system as shown in Fig. 1, the displacement and velocity of the cart under the Coulomb plus Viscous friction model are shown in Fig. 11.

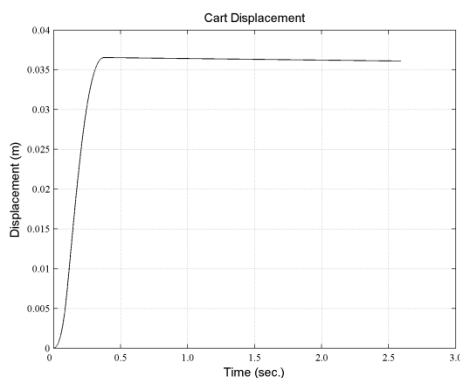


Figure 11. Cart displacement under Coulomb+viscous friction model

From Fig. 11, the cart velocity under the Coulomb plus viscous friction model does not change to negative. The cart displacement under the Coulomb plus viscous friction model does not decrease any more. At the same time, the improved friction model can also makes the cart drives to the same displacement with the previous friction models, without any inverse motion, which is consistent with the physical phenomena.

This paper has completed the following tasks

- Studied the friction phenomena and investigated switching between static and dynamic friction models.
- Proposed two selection criterions of the friction models.
- Simulated the spring-steel block system.
- Did the physical experiment.

- Got the most suitable friction model for the spring-steel mass block system as shown in Fig. 5 and the pendulum-driven cart system as shown in Fig. 1.

In conclusion, the selected friction model considers the switching between dynamic and static friction, and makes the pendulum-driven cart system move in the positive direction without any inverse motion.

REFERENCES

- [1] Ernest Rabinowicz, "Friction and wear of materials," 2nd ed. Wiley-Interscience, 1995, pp. 65-79.
- [2] C. Canudas de Wit, H. Olsson, K. J. Astrom and P. Lischinsky, "A new model for control of systems with friction," IEEE transactions on automatic control, vol. 40, No.3, March 1995, pp. 419-425.
- [3] Hongyi Li, Katsuhisa Furuta, Chernousko, F.L." Motion generation of the capsbot using internal force and static friction," presented at the 2006 IEEE Conference, Decision and Control, San Diego, CA, Dec. 13-15, 2006, pp. 6575-6580.
- [4] M. Nazmul Huda, Hong-Nian Yu and Samuel Olive Wane,"Self-contained capsbot propulsion mechanism," International Journal of Automation and Computing, Vol. 8, No. 3, August 2011, pp. 348-356.
- [5] Y. Liu, H. Yu, and T. C. Yang, "Analysis and control of a capsbot", proceedings of the 17th world congress, the international federation of Automatic Control, Seoul, Korea, July 6-11, 2008.
- [6] H Yu, Y Liu, and T Yang. "Closed-loop tracking control of a pendulum-driven cart-pole underactuated system," Journal of System and Control Engineering, vol. 222, no.2. pp. 109-125, 2008.
- [7] Y Liu, H Yu, and B Burrows. "Optimization and control of a pendulum-driven cart-pole system," In proceedings of the IEEE International Conference on Networking, sensing and control, London. April 2007, pp. 151-156.
- [8] H. Olsson, K.J. Astrom, C. C. de Wit, M. Gafvert, P. Lischinsky, Friction models and friction compensation. Eur. J. Control, Vol. 4, No. 3. 1998, pp. 176-195.
- [9] Brian Armstrong-Helouvy, Pierre Dupont and Carlos Canudas de Wit, A survey of models, analysis tools and compensation methods for the control of machines with friction. Automatica, Vol. 30, No. 7,1994, pp. 1083-1138.
- [10] P.R. Dahl, "A solid friction model," Belvoir Defense Technical Information Centre, May 1968.
- [11] D. A. Haessig, Jr and B. Friedland, "On the modelling and simulation of friction," J. Dyn. Sys., Meas, Control, Vol. 113, Issue. 3, September 1991, pp. 354-362.
- [12] Paul Breedveld, Annemarie Y. Diepenbroek, Ton van Lunteren. "Real-time simulation of friction in a flexible space manipulator," ICAR 1997, Monterey, CA, July 7-9, 1997.
- [13] J. Courtney-Pratt and E. Eisner. "The effect of a tangential force on the contact of metallic bodies," in proceeding of the Royal Society, Vol. A238, 1957, pp. 529-550.
- [14] Armstrong-Helouvy, Brian, "Control of machines with friction," The Springer International Series in Engineering and Computer Science, 1 Edition, 1991, pp. 10.
- [15] O. Reynolds, "On the theory of lubrication and its application to Mr. Beauchamp Tower's experiments, including an experimental determination of the viscosity of olive oil," transactions of the Royal Society of London Proceedings Series 1, 1886, pp. 157-234.
- [16] K.J. Astrom and C. Canudas-de-Wit, "Revisiting the LuGre model," IEEE Control Systems Magazine 28, June 2006, pp. 101-114.
- [17] American Society for Metals, ASM Handbook, Vol. 18, Lubrication, and Wear Technology.
- [18] Karnopp, D. 1985, Computer simulation of stick-slip friction in mechanical dynamical systems. Journal of Dynamic Systems, Measurement, and Control, 107, 100-103.